K&C Science Report – Phase 2
High-grade forest and land-cover mapping in the boreal zone

Christian Thiel
Friedrich-Schiller-University Jena, Loebdergraben 32, Christian.Thiel@uni-jena.de
Christiane Schmullius
Friedrich-Schiller-University Jena, Loebdergraben 32, c.schmullius@uni-jena.de

***Abstract*—Original idea of the phase 2 proposal was to use the information contained in the winter coherence additionally to the backscatter for land cover mapping in the boreal zone. This idea was based on the very promising results of phase one. So far, the data base in terms of coherence data strips could not be provided. However, the whole approach is pending and might be accomplished at phase 3, at least for a smaller demonstration area. Thus, phase 2 had to concentrate on a different topic. New topic was to investigate the use of interferometric coherence for forest biomass estimation. This study was accomplished by using standard FBS/FBD SLC data provided by JAXA. Major results are: 1.) Winter coherence contains much information on forest stem volume, even if temporal baseline is larger than one cycle; 2.) For winter coherence no spatial baseline dependency is evident; 3.) Surprisingly the coherence for dense forest is larger in summer than in winter; 4.) At forest scattering processes in summer and winter are different; 5.) The scattering phase centre drops in winter.**

***Index Terms*—ALOS PALSAR, K&C Initiative, Forest Theme, above-ground biomass, Coherence, Baseline effect**

I. INTRODUCTION

A. Background of investigating multi-seasonal coherence

The great potential of SAR data for forestry applications has been clearly demonstrated by a remarkable number of studies. While techniques aiming at forest cover and forest disturbance mapping (e.g. logging, forest fire, and wind damage) almost reached operational stage (at least in the boreal zone) [1, 2, 3, 4, 5, 6, 15], the estimation of forest biomass still struggles with problems related to saturation and considerable uncertainties [7, 8, 9]. However, the extension of the timeline (multitemporal data) proved having the potential to overcome these shortcomings [10, 11, 12, 13, 14, 19].

If SAR data are used in the boreal zone, the extreme seasonality needs to be considered throughout the SAR data exploration [13, 14]. During winter the trees are frozen and thus, in particular at L-band, almost transparent for the incoming radar wave. The backscatter generated by the trees as well as the contrast between forest and non-forest is significantly reduced [18]. In winter, the environmental conditions are very stable. Due to the very low temperatures, the snow is very dry and does hardly impact the scattering. As the soil is also frozen, soil moisture changes do not appear. With regards to coherence, these circumstances lead to very low temporal decorrelation. Even long temporal baselines of 44/46 days (JERS-1/ALOS PALSAR) do not necessarily cause problems due to temporal decorrelation [6, 11]. From a number of studies it is evident that in particular coherence images acquired during winter do have great potential for forest biomass estimation [10, 11, 12].

The thawing phase (spring time) however was recognised being the most unsuitable time for coherency based forest parameter retrieval [11, 14]. Due to the very unstable conditions in terms of snow cover and soil moisture coherence is almost completely lost. During midsummer major sources of temporal decorrelation are rainfall (changing soil moisture and interception water) and wind. Thus, in general repeat pass coherence of forest is assumed being much smaller compared to mid-winter.

The above mentioned hypothesises on the seasonal variation of repeat-pass coherence are substantiated by a number of ERS-1/2 Tandem coherence studies [10, 12, 13, 14]. However, not much is known about the seasonality of repeat-pass L-band coherence. There is one study by [11] on multitemporal JERS repeat-pass coherence for stock volume estimation in Siberia. However, [11] clearly focus on winter coherence, as the database did not allow a thorough multi-seasonal investigation.

B. The content

Altogether 16 sites have been in the focus of this study. Those sites were covered by 8 (sometimes more than one site is covered by one frame) frames and altogether 87 images. All summer-summer and winter-winter (and some summer-winter) combinations of SLC pairs have been implemented for coherence estimation ending up with a number of almost 300 coherence images. The results can be summarised as follows:

1.) Winter coherence contains much information on forest stem volume, even if temporal baseline is large

2.) No spatial baseline dependency is evident for winter coherence

3.) Surprisingly the coherence for dense forest is larger in summer than in winter
4.) At forest scattering processes differ in summer and winter
5.) The scattering phase centre drops in winter.

II. Description of your project

A. Study area

The study area is located in Central Siberia, Russia (see Fig. 1) and features the administrative compartments Irkutsk Oblast and Krasnoyarsk Kray. The Middle Siberian Plateau in the southern part of the territory is characterised by hills up to 1,700 m. The northern part is flat with heights up to 500 m. Taiga forests (spruce, birch, larch, pine, aspen etc.) dominate and cover ca. 80% of the region. The region exhibits continental climatic conditions. The yearly amount of precipitation is generally below 450 mm; the winters are very cold and dry, the summers are warm; most of the precipitation occurs in summer. The whole territory is characterised by extreme land cover changes caused by forest fires and logging.

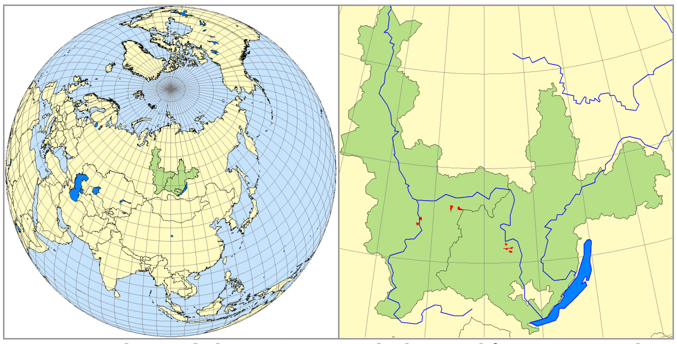

Figure 1. Study area (light green) in Central Siberia and forest inventory data; Area covered by right image ca. 2,000 km × 2,000 km

B. Relevance to the K&C drivers

Primary objective is to investigate interferometric coherence data with regards to their potential for forest stem volume estimation in the boreal zone. Basing on these findings an estimation/monitoring approach will be developed in phase 3. Thus, the objective is very much related to all of the three C's **C**onventions, **C**arbon and **C**onservation. Additional and very important scientific objective is to understand the seasonal differences of coherence.

C. Work approach - summary

Besides the impact of the environmental conditions (seasonality) also the impact of the spatial baseline for the SLC pairs has to be considered. Thus, the spatial baseline effect was investigated for dense forest, where it is expected having the greatest impact. To support the clarification of the coherence behaviour an investigation of the INSAR phase has been added to the work plan.

Considering all required framing conditions the data has been investigated with regards to correlation between coherence and stem volume, point of saturation, average site coherence, and average dense forest coherence.

D. Satellite data and processing

Tab. 1 summarises the implemented PALSAR data. Only 8 frames were required as some of the frames cover more than one test site. In general, FBS was acquired in winter and FBD in summer. For the coherence estimation level 1.1 FBS/FBD scenes were applied. Interferometric processing consisted of SLC data co-registration at sub-pixel level, slope adaptive common-band filtering in range [16, 17], and common-band filtering in azimuth. The interferograms/ coherence images were generated using 10x20 looks for FBS and 10x40 looks for FBD data. The coherence images were orthorectified using SRTM elevation data.

TABLE I
Implemented PALSAR data; Cursive: unfrozen conditions, Bold: FBD, Standard: FBS, frozen conditions

Chunsky N	**Chunsky E**	**Primorsky**	**Bolshe**
T475/F1150	T473/F1150	T466/F1110	T481/F1140
(Track/Frame)	30dec06	18jan07	28dec06
	14feb07	05mar07	12feb07
20jun07	***02jul07***	***21jul07***	***15aug07***
05aug07	***17aug07***	***05sep07***	***30sep07***
20sep07	***02oct07***	***21oct07***	
	17nov07		
05nov07			
21dec07			31dec07
05feb08	02jan08	21jan08	15feb08
22mar08	17feb08		
07may08			
22jun08			
07aug08	***04jul08***		***02jul08***
	19aug08		***17aug08***
	04jan09		02jan09
	19feb09		17feb09
Shestakovsky	**Nizhne-Udinsky**	**Irbeisky**	**Hrebtovsky**
T0463/F1130	T0471/F1100	T0478/F1100	T0468/F1190
13jan07	11jan07		06jan07
28feb07	26feb07		21feb07
16jul07	***14jul07***		***09jul07***
31aug07		***10aug07***	***24aug07***
16oct07	***14oct07***		***09oct07***
16jan08		**10nov07**	09jan08
02mar08	29feb08	26dec07	24feb08
17apr08		10feb08	***11jul08***
18jul08	***16jul08***	***27jun08***	***26aug08***
02sep08	***31aug08***	***12aug08***	
18jan09	16jan09	28dec08	11jan09
05mar09	03mar09	12feb09	26feb09
21jul09		***30jun09***	***14jul09***
05sep09		***15aug09***	***29aug09***
21oct09		***30sep09***	***14oct09***

Tab. 2 - Tab. 9 exhibit the perpendicular baselines derived using state vector data. N/a values denote that for the respective image pair no coherence was computed. This applies to some summer-winter coherence combinations and some pairs with presumably very large perpendicular baseline due to orbit correction manoeuvres.

TABLE 2. PERPENDICULAR BASELINES T475/F1150

	20jun07	05aug07	20sep07	05nov07	21dec07	05feb08	22mar08	07may08	22jun08
05aug07	343	0							
20sep07	430	86	0						
05nov07	-1107	-763	-676	0					
21dec07	-1159	-815	-729	52	0				
05feb08	-2049	1705	-1618	942	889	0			
22mar08	-2472	560	-2041	1364	1311	422	0		
07may08	3032	2688	2601	1925	1872	983	560	0	
22jun08	n/a	n/a	n/a	n/a	n/a	n/a	n/a	-3749	0
07aug08	n/a	n/a	n/a	n/a	n/a	n/a	n/a	-7810	-4059

TABLE 3. PERPENDICULAR BASELINES T473/F1150

	30dec06	14feb07	02jul07	17aug07	02oct07	17nov07
14feb07	1406	0				
02jul07	n/a	n/a	0			
17aug07	n/a	n/a	272	0		
02oct07	n/a	n/a	668	396	0	
17nov07	3505	2099	1146	874	478	0
02jan08	-3636	-2229	n/a	n/a	n/a	-129
17feb08	-4668	-3261	n/a	n/a	n/a	-1161
04jul08	n/a	n/a	-1265	-1538	-1934	-2412
19aug08	n/a	n/a	-4661	-4934	-5330	-5808
04jan09	-534	-1940	n/a	n/a	n/a	4040
19feb09	94	-1311	n/a	n/a	n/a	3411

	02jan08	17feb08	04jul08	19aug08	04jan09
17feb08	1031	0			
04jul08	n/a	n/a	0		
19aug08	n/a	n/a	-3394	0	
04jan09	-4170	-5203	n/a	n/a	0
19feb09	-3541	-4573	n/a	n/a	628

TABLE 4. PERPENDICULAR BASELINES T466/F1110

	18jan07	05mar07	21jul07	05sep07	21oct07
05mar07	1630	0			
21jul07	2472	842	0		
05sep07	2703	1073	-230	0	
21oct07	3139	1509	-666	-435	0
21jan08	3953	2324	-1481	-1251	-815

TABLE 5. PERPENDICULAR BASELINES T481/F1140

	28dec06	12feb07	15aug07	30sep07	31dec07	15feb08	02jul08	17aug08	02jan09
12feb07	1278	0							
15aug07	2450	1171	0						
30sep07	2880	1601	430	0					
31dec07	3473	2194	-1023	-593	0				
15feb08	4576	3298	-2127	-1697	1103	0			
02jul08	962	-315	-1487	1918	-2511	-3615	0		
17aug08	-2463	-3741	-4914	5343	-5939	-7044	3425	0	
02jan09	-652	-1930	n/a	n/a	-4127	-5232	1614	-1810	0
17feb09	50	-1227	n/a	n/a	-3424	-4528	911	-2514	703

TABLE 6. PERPENDICULAR BASELINES T0463/F1130

	13jan07	28feb07	16jul07	31aug07	16oct07	16jan08	02mar08	17apr08	18jul08
28feb07	1610	0							
16jul07	n/a	n/a	0						
31aug07	n/a	n/a	337	0					
16oct07	n/a	n/a	836	500	0				
16jan08	4092	2482	n/a	n/a	n/a	0			
02mar08	4857	3248	n/a	n/a	n/a	765	0		
17apr08	5312	3702	n/a	n/a	n/a	1220	455	0	
18jul08	n/a	n/a	-1303	-1640	-2140	n/a	n/a	n/a	0
02sep08	n/a	n/a	-4421	-4759	-5260	n/a	n/a	n/a	-3119
18jan09	-207	-1817	n/a	n/a	n/a	-4301	-5067	-5523	n/a
05mar09	320	-1291	n/a	n/a	n/a	-3774	-4540	-4996	n/a
21jul09	n/a	n/a	-1689	-2027	-2527	n/a	n/a	n/a	-386
05sep09	n/a	n/a	-1064	-1401	-1901	n/a	n/a	n/a	239
21oct09	n/a	n/a	-599	-937	-1437	n/a	n/a	n/a	704

	02sep08	18jan09	05mar09	21jul09	05sep09	21oct09
18jan09	n/a	0				
05mar09	n/a	-527	0			
21jul09	2731	n/a	n/a	0		
05sep09	3357	n/a	n/a	626	0	
21oct09	3821	n/a	n/a	1090	464	0

TABLE 7. PERPENDICULAR BASELINES T0471/F1100

	11jan07	26feb07	14jul07	14oct07	29feb08	16jul08	31aug08	16jan09	03mar09
26feb07	1650	0							
14jul07	n/a	n/a	0						
14oct07	n/a	n/a	884	0					
29feb08	4862	3213	n/a	n/a	0				
16jul08	n/a	n/a	-1293	-2177	n/a	0			
31aug08	n/a	n/a	-4419	-5303	n/a	-3127	0		
16jan09	-102	-1753	n/a	n/a	-4968	n/a	n/a	0	
03mar09	364	-1287	n/a	n/a	-4501	n/a	n/a	466	0

TABLE 8. PERPENDICULAR BASELINES T0478/F1100

	10aug07	10nov07	26dec07	10feb08	27jun08	12aug08	28dec08	12feb09	30jun09
10nov07	1157	0							
26dec07	n/a	129	0						
10feb08	n/a	-879	1008	0					
27jun08	-1072	n/a	n/a	n/a	0				
12aug08	-4725	n/a	n/a	n/a	-3651	0			
28dec08	n/a	4261	-4134	-5142	n/a	n/a	0		
12feb09	n/a	3405	-3278	-4286	n/a	n/a	855	0	
30jun09	-1479	n/a	n/a	n/a	-407	3243	n/a	n/a	0
15aug09	-1407	n/a	n/a	n/a	-335	3315	n/a	n/a	72
30sep09	-848	n/a	n/a	n/a	225	3875	n/a	n/a	632

	15aug09
30sep09	560

TABLE 9. PERPENDICULAR BASELINES T0468/F1190

	06jan07	21feb07	09jul07	24aug07	09oct07	09jan08	24feb08	11jul08	26aug08
21feb07	1608	0							
09jul07	n/a	n/a	0						
24aug07	n/a	n/a	175	0					
09oct07	n/a	n/a	629	455	0				
09jan08	3978	2371	n/a	n/a	n/a	0			
24feb08	4866	3259	n/a	n/a	n/a	888	0		
11jul08	n/a	n/a	-1388	-1562	-2017	n/a	n/a	0	
26aug08	n/a	n/a	-4810	-4983	-5439	n/a	n/a	-3421	0
11jan09	-427	-2035	n/a	n/a	n/a	-4407	-5296	n/a	n/a
26feb09	122	-1486	n/a	n/a	n/a	-3858	-4747	n/a	n/a
14jul09	n/a	n/a	-1356	-1530	-1985	n/a	n/a	32	3451
29aug09	n/a	n/a	-957	-1131	-1586	n/a	n/a	431	3850
14oct09	n/a	n/a	-698	-872	-1327	n/a	n/a	690	4109

	11jan09	26feb09	14jul09	29aug09	14oct09
26feb09	549	0			
14jul09	n/a	n/a	0		
29aug09	n/a	n/a	399	0	
14oct09	n/a	n/a	658	259	0

E. Ground reference data

With regards to the coherence investigation forest inventory data was used for the sites Bolshe Murtinsky NE and SE, Chunsky N and E, Primorsky N, E, S, and W, Hrebtovsky S, and NE, Nishni Udinsky, Irbeisky E, N, W, and CTR and Shestakovsky. The forestry data contains lots of parameters, so far only stem volume, stand ID, and relative stocking have been considered. The data was provided digitally (vector data).

Some specific characteristics of the forestry data base had to be considered: i) Only trees with economic relevance are included (stem diameter > 8 cm etc.), ii) In places high heterogeneity within forest stands was detected (e.g. only partly logged), iii) Polygons are inaccurate – the misregistration is partially more than 100 m, iv) The forest information is outdated (GIS layer 15 years old, information contained in GIS even older, thus potentially new clear-cuts, growth and regrowth of forest). To overcome some of these issues the following strategies have been applied: i) Buffering polygon information, ii) Excluding forest stands which have been logged or burned during last 10 years (detection by means of HR EO data, creation of list with obsolete stands), iii) Exclusion of stands with very high variance of coherence, iv) Excluding stands smaller than 2 ha, v) Excluding outliers, the threshold was set to 2 standard deviations.

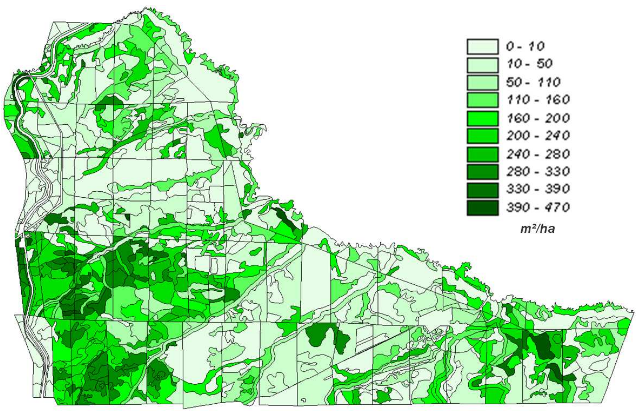

Figure 2. Example for forest inventory data (Chunsky E)

F. *Meteorological Data*

The meteorological network in Siberia is not very dense. Thus, the distance between the forest inventory data sites and the corresponding meteorological station can be greater than 200 km. Meteorological data was collected for the stations Bolshaja Murta (93°08'E, 56°54'N), Bogucany (97°27'E, 58°23'N), Tulun (100°36'E, 54°36'N), and Bratsk (101°45'E, 56°17'N). Due to spatial constraints the data is not provided in this paper. The reader is referred to [18]. All meteorological data was gathered from the webpages www.wunderground.com and www.wetteronline.de. It was collected for the acquisition date of the SAR data. Regarding precipitation also a sum for the 3 and 7 days before the acquisition (including the acquisition day) was determined.

In general, typical weather conditions have been observed. Temperatures were far below freezing point during winter acquisitions and well above 0°C during summer. No or only little precipitation was measured at the acquisition dates and the days before. Wind did not play a major role. Furthermore, no remarkable snow melt occurred during the winter cycles.

III. Results and Summary

A. *Investigation of impact of spatial baseline*

With regards to the earth's surface and its objects coherence is determined by temporal and spatial decorrelation. Temporal decorrelation is cause by natural and human induced changes resulting in differing dielectric and geometric properties when comparing both SLC images. The prediction of temporal decorrelation is hardly possible, thus, with regards to stem volume estimation it introduces unwanted noise. Spatial decorrelation is caused by the differing viewing geometry of both SLC images which introduces a wave number shift, which in turn decreases the coherence. For vegetation-free terrain this shift can be predicted and a correction (common band filtering) of this component of spatial decorrelation is possible. However, in areas with dense and high vegetation such as forests the vertical assembly of scatterers introduce a second component of decorrelation, which is referred to volume decorrelation. It is depending on the perpendicular baseline and the vertical distribution of the scatterers. If the vertical distribution of the scatterers is not known, which is mostly the case, this component is not predictable. Thus, the impact of spatial baseline for dense forest was empirically investigated first.

Within this study the average forest coherence was computed for each coherence image and test site. All forest stands with a stem volume of 250 m³/ha – 350 m³/ha were considered. The average forest coherence was plotted against the perpendicular baseline (see Fig. 3-6).

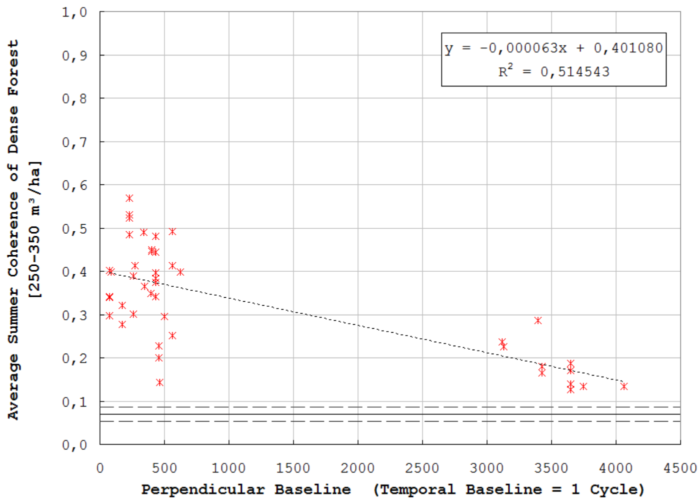

Figure 3. Interferometric summer coherence of dense forest as function of spatial baseline – temporal baseline = 46 days. Horizontal lines denote coherence (and its standard deviation) for decorrelated data

Fig. 3 depicts the interferometric coherence of dense forest as function of spatial baseline for summer coherence data with a temporal baseline of 46 days. First of all it becomes apparent that the ALOS orbit is in a stable tube and the baselines range from 100 m to 600 m only. However, for some SLC pairs the perpendicular baseline is much larger (3,100 – 4,100 m). The large baselines are the result of orbit correction manoeuvres which are in general required every second year.

With regards to coherence a wide spread, even for the same spatial baseline, is apparent. This spread is mainly caused by the varying temporal decorrelation. However, comparing small and large baseline forest coherence, a clear decrease with baseline is obvious. Thanks to the well managed orbit no intermediate baselines (~2000 m) can be found for 46 day summer coherence, even though these would help interpreting the impact of the spatial baseline.

As zero reference the coherence for completely decorrelated images is represented by a horizontal line (0.070); the dashed lines represent the respective standard deviation. These parameters have been computed by processing random data. Additionally the results have been compared with the coherence for water bodies (0.076) – both measures were in good accordance. The expected value of coherence for uncorrelated datasets is a function of the number of independent looks – thus it can also be computed without running the coherence processor. However, the application of the common band filter diminishes the number of independent looks. Thus, the actual look number is unknown (not provided by the gamma software).

When not considering large baselines the above Fig. 3 becomes as follows (Fig. 4):

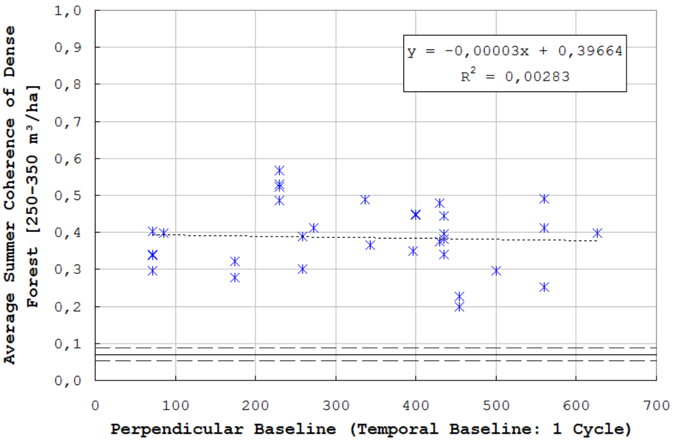

Figure 4. Interferometric summer coherence of dense forest as function of spatial baseline – temporal baseline = 46 days, small perpendicular baselines

By showing small baseline data only no specific trend is visible. Again, the variations of coherence of around 0.3 are most likely driven by varying temporal decorrelation. Thus, considering only these small baseline data sets for further investigation, baseline effects can be neglected.

By increasing the temporal baseline a much larger number of potential SLC pairs results in a much larger variety of perpendicular baselines:

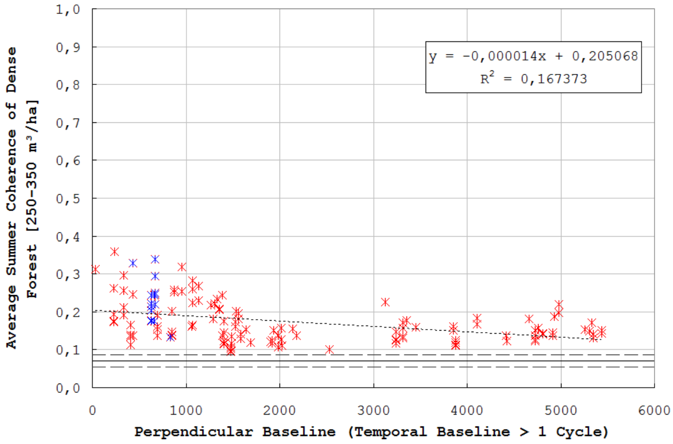

Figure 5. Interferometric summer coherence of dense forest as function of spatial baseline – temporal baseline = 72 days (blue) and > 72 days (red), all perpendicular baselines

By examining Fig. 5 one must mind that the summer coherence for forest is depicted for a large variety of temporal baselines. They range from 72 days to more than 2 years. Thus, the potential of having temporal effects is also large. Still, all measures are above the minimum expected coherence for random data, i.e. some remaining forest coherence can be found in each image. Even though this investigation was accomplished for dense forest, there might appear gaps in the canopy which result in some residual coherence.

As expected, the average coherence for small spatial baselines is reduced against the 46 day coherence. Furthermore, having also intermediate perpendicular baselines available, the clear trend of decreasing coherence with increasing baselines becomes apparent. In particular between 1,000 m and 2,000 m this tendency is obvious. This effect must be considered during the following data interpretation.

Analogue to the summer data the same plots were generated for winter coherence images. Fig. 6 depicts the result for 46 day coherence.

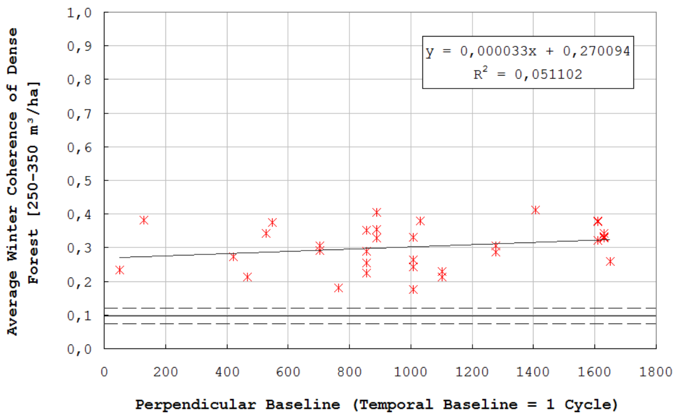

Figure 6. Interferometric winter coherence of dense forest as function of spatial baseline – temporal baseline = 46 days

In comparison to 46 day summer data we find larger perpendicular baselines in winter. The overall coherence for dense forest is surprisingly about 0.1 lower than in summer. The same applies to the variability of the winter coherence of forest. This can be explained by the reduced variations of the temporal decorrelation in winter (more stable conditions).

Of particular interest is the fact, that even over the large range of baselines no general trend of coherence is evident. Thus, working with 46 day winter coherence data, baseline effects can be neglected.

Fig. 7 summarises the baseline impact on coherence with large temporal baselines of 72 days (blue) and > 72 days (red). The latter one refers to inter annual coherence with temporal baselines greater than 2 years. The largest spatial baselines are around 5,500 m, thus we find about the same baseline distribution as for the summer coherence data (Fig. 5). First of all, again a decrease of forest coherence with increasing temporal distance between the two acquisitions is evident. We find an average forest coherence of 0.3 for 46 day coherence, of 0.25 for 72 day coherence, and of 0.2 for greater temporal baselines.

Secondly and even more interesting, again there is no impact of spatial baseline on forest coherence. Although some of the measures are quite close to the noise level, we find sufficient points with no complete decorrelation. Also these measures show no impact of the spatial baseline. Thus, again, we find a different behaviour of winter forest coherence with regards to spatial baseline. Thus, also working with large temporal baseline winter coherence data, spatial baseline effects can be neglected.

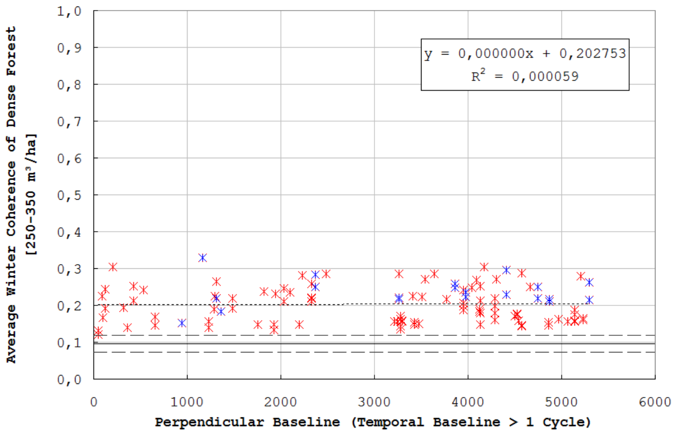

Figure 7. Interferometric winter coherence of dense forest as function of spatial baseline – temporal baseline = 72 days (blue) and > 72 days (red)

B. *Methodology of coherence analysis*

The correlation analysis between stem volume and interferometric coherence is conducted on forest stand level. Thus, coherence was averaged for each stand. The standard deviation was also computed stand wise and was used as exclusion criterion (all stands with $STD_{COH} > 0.1$ are excluded). All remaining forest stands have been considered as separate entities and the empirical model was fit to the whole set of entities. In the next step an empirical model by [19] was fit to the data (Eq. 1):

$$\gamma_{vol} = ae^{\frac{-vol}{c}} + b\left(1 - e^{\frac{-vol}{c}}\right) \qquad (1)$$

In this model γ_{vol} is the interferometric coherence, *vol* refers to stem volume, and *a, b,* and *c* are empirical coefficients. After fitting the model outliers have been removed and the model was fit again (only one iteration). R² and the coefficients of the empirical model are provided as well.

C. *Results of coherence analysis*

The coherence was estimated for temporal baselines of 46 days up to two years. The individual images have been acquired during summer and winter. Depending on temporal baseline and combination of acquisition season the coherence images feature various characteristics.

Fig. 8 & 9 demonstrate the typical behaviour of 46 day winter-winter coherence. Clear-cuts and forest are well distinguishable; coherence is high for low biomass patches and decreases with increasing stem volume. This relationship can be well described by means of the empirical model; the coefficient of determination is fairly high.

Figure 8. Coherence for northern part (~20 km x 10 km) of Chunsky N (21dec07_05feb08), average coherence 0.42, B_{perp} = 889 m

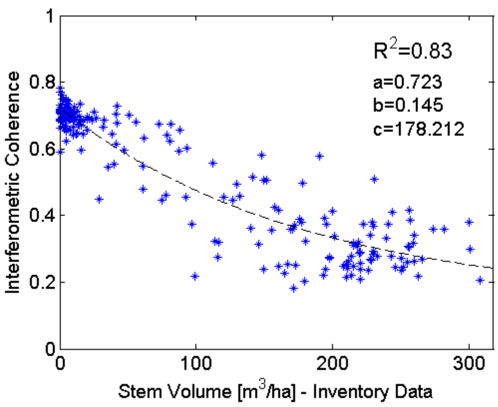

Figure 9. Scatterplot for Chunsky N (21dec07_05feb08)

Fig. 10 & 11 demonstrate the same issue, this time however for winter-summer coherence and a longer temporal baseline. Besides the fact that the overall scene coherence is very low (0.16), and the image is very noisy, only minor information can be gathered from this image. It is even difficult to detect forest free patches. From the scatterplot (Fig. 5) it gets clear that only very low stem volume forest patches can generate coherence above the noise level.

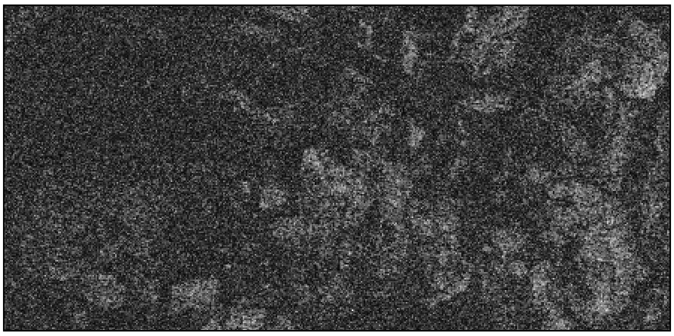

Figure 10. Coherence for northern part (~20 km x 10 km) of Chunsky N (05feb08_20jun07), average coherence 0.16, B_{perp} = -2,049 m

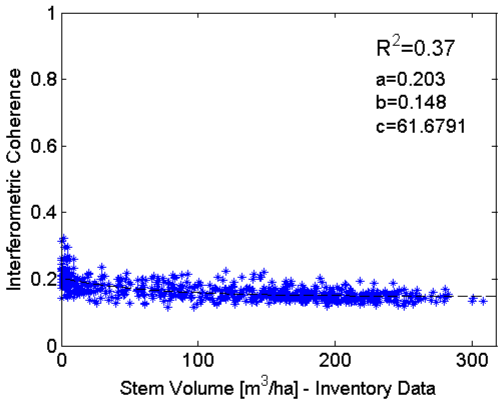

Figure 11. Scatterplot for Chunsky N (21dec07_05feb08)

Fig. 12 & 13 provide an example for 46 day summer-summer coherence. Remarkable is the overall high scene coherence, even for high stem volume forest.

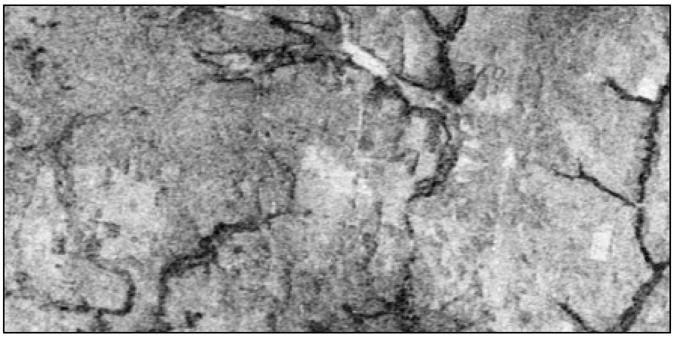

Figure 12. Coherence for northern part (~20 km x 10 km) of Chunsky N (05aug07_20sep07), average coherence 0.46, B_{perp} = 86 m

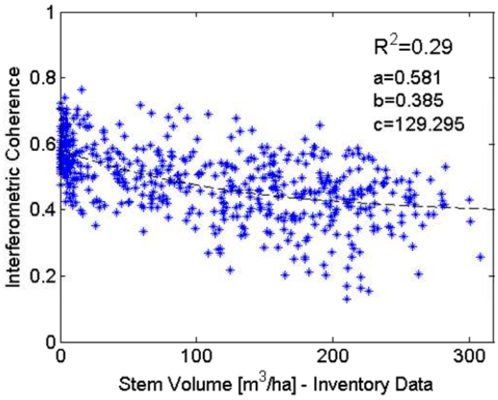

Figure 13. Scatterplot for Chunsky N (05aug07_20sep07)

By viewing Fig. 12 forested and non-forested areas can hardly be discriminated (compare to Fig. 8). Still, with increasing stem volume the coherence decreases, the slope (Fig. 13) however is much smaller compared to the winter-winter example. Additionally, the coherence seems to be much more scattered. In summary, 46 day summer coherence is not very sensitive to stem volume. In fact, for most of the coherence images there was hardly any trend of decreasing coherence with increasing stem volume. Actually, some examples with reverse trend were found (see Fig. 14 for one and later section for discussion).

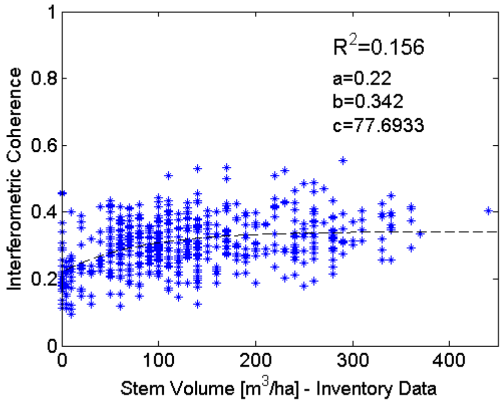

Figure 14. Scatterplot for Primorsky W (05sep07_21oct07), B_{perp} = -435 m

By increasing the temporal baseline (Fig. 15 & 16) the observed characteristics remain the same. Again, winter-winter coherence is favourable against summer-summer coherence for stem volume retrieval, although R^2 is reduced and saturation occurs at lower stock volume. Although not visible in example provided by Fig. 16, an increment of the temporal (and spatial) baseline of summer-summer coherence can lead to an improvement of the stem volume – coherence relationship (see section below). In particular the perceptibility of non-forest areas is increased.

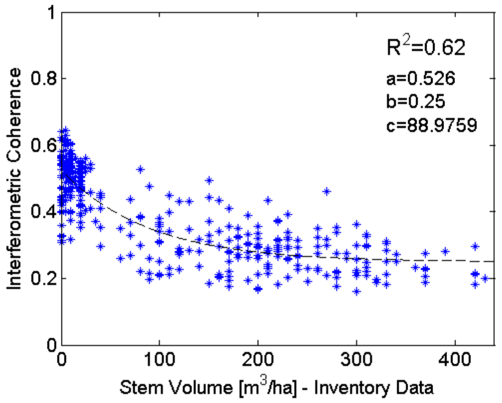

Figure 15. Scatterplot for Chunsky E (30dec06_02jan08), B_{perp} = -3,636m

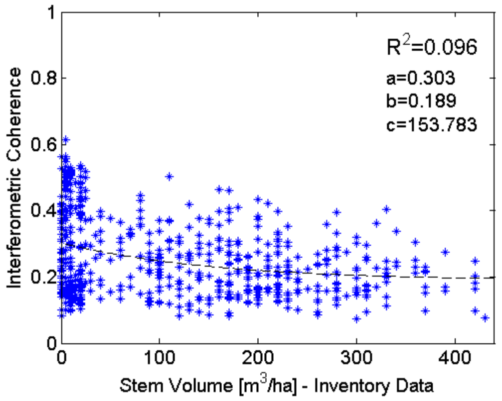

Figure 16. Scatterplot for Chunsky E (02jul07_04jul08), B_{perp} = -1,265 m

D. *Summary of coherence analysis*

Basing on the baseline effect investigation baseline effects will be neglected for all winter-winter combinations. With regards to summer-summer SLC pair combinations only pairs with a perpendicular baseline smaller 640 m have been considered, which also allows the negligence of baseline effects with regards to volume decorrelation. This assumption is yet not valid for summer pairs with baselines larger 1 km. This report does not consider the baseline induced reduction of forest coherence. This will be focus of future work. Yet, the large database allows some general conclusions.

Several statistical parameters have been computed to describe the characteristics of the coherence data (compare Fig. 17-19). These parameters have been computed for each considered coherence image. To summarise the results, the coherence images are grouped by season and temporal baseline, expressed as orbit cycles (one cycle equals 46 days):

- ww1: winter-winter coherence, 1 cycle
- ss1: summer-summer coherence, 1 cycle
- ww2-3: winter-winter coherence, 2-3 cycles
- ss2-3: summer-summer coherence, 2-3 cycles
- ww>3: winter-winter coherence, >3 cycles
- ss>3: summer-summer coherence, >3 cycles
- sw>0: summer-winter coherence, all cycles

For each group mean, minimum, and maximum are provided. The reader must be aware that for some of the groups only a very limited number of coherence images was available. As not all results can be presented here, a selection of parameters is provided for Chunsky North (Fig. 17 – Fig. 19). For some further results see [18].

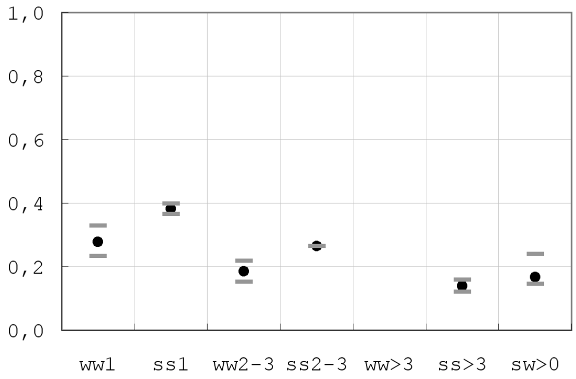

Figure 17. Average coherence for stem volume 250-350 m³/ha (Chunsky N)

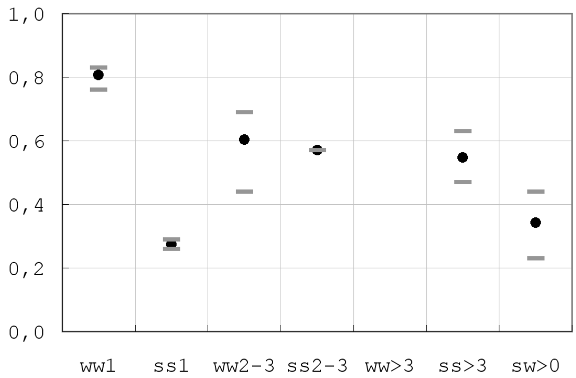

Figure 18. R^2 for stem volume vs. coherence (Chunsky N)

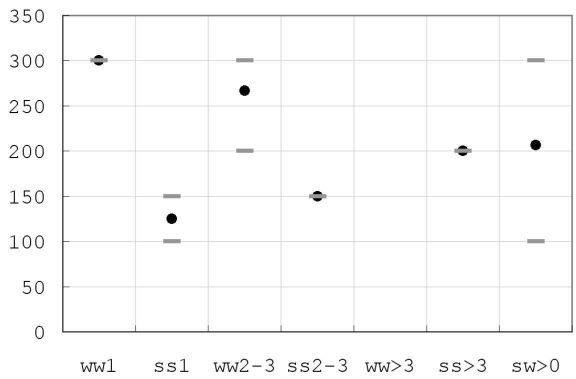

Figure 19. Saturation level [m³/ha] (Chunsky N)

Basing on all investigated data the following summary of the statistical analysis can be given:

i) Consecutive cycles (temporal baseline = 1 cycle):

- The averaged summer-summer coherence of a complete scene and of dense forest in general well exceeds winter-winter coherence;

- R^2 (stem volume vs. coherence) is not depending on mean coherence (of complete scene & dense forest);
- Saturation occurs at very low stem volume for summer-summer coherence and close to maximum biomass for winter-winter coherence;
- Increasing stem volume always results in decrease of winter-winter coherence, for summer-summer coherence a reversal of this relationship was observed four times;
- For summer-summer coherence in general weak correlation (stem volume vs. coherence) was observed, the spread of coherence measures per stem volume class is much higher than in winter;

ii) For temporal baseline of 2-3 cycles (intra season):

- Winter-winter coherence in general behaves as the consecutive cycle coherence, average coherence values, R^2, and saturation are slightly decreased;
- Summer-summer coherence also decreases for complete scene and for dense forest, however R^2, and saturation can improve compared to consecutive cycle coherence

iii) For temporal baseline of > 3 cycles (inter season):

- Winter-winter coherence behaves as 2-3 cycle winter coherence – no remarkable change of average coherence values, R^2, and saturation;
- Summer-summer coherence in general further decreases (for complete scene and for dense forest); R^2, and saturation can improve or degrade against 2-3 cycle coherence – seemingly strongly dependent on environmental conditions

iv) Summer-winter coherence, all temporal baselines:

- In general almost complete decorrelation was observed, hardly any practical information can be gathered – very few images (Chunsky North) could be useful (very low sensitivity to stem volume, yet very low intra-stem-volume-class variation).

E. Phase analysis

The results of the above coherence analysis are in some part very surprising as they deviate from recent theory. In particular the high coherence for dense forest in summer (greater than in winter) and the inverse trends of the stock volume – coherence relationship during snow melt can be hardly explained with recent theory.

As one major reason for the decreased decorrelation in summer the decrease of volume decorrelation needs to be considered (see discussion paragraph), the penetration depth into the canopy is investigated. The higher the penetration depth, the higher is the vertical extension of the scattering relevant volume and thus the higher is the volume decorrelation. The difference of penetration depth between summer and winter data is derived from the INSAR phase offsets at forest/clear-cut edges (wanes).

The generation of the interferograms followed the same steps as described above: SLC data co-registration at sub-pixel level, slope adaptive common-band filtering in range, and common-band filtering in azimuth. The filtering of the flattened interferogram was conducted by means of the adaptive spectral filter as proposed by [20] applying the following parameterisation: exponent for non-linear filtering alpha = 0.5, filtering FFT window size = 32, coherence parameter estimation window size = 7.

Areas with coherence less than 0.95 and with slopes steeper than 5° were masked out. This step was required to include only low noise phase and minimise the topographic effects in this study. At this point it must be emphasized, that only SRTM elevation data was available as height reference. In Fig. 20 the effect of forest on the elevation data can be identified. As both, the penetration depth at C-band during SRTM campaign and the exact tree heights are not known, the methods of investigation are limited. For simplicity, only those wanes were considered, were the SRTM data features greater elevation for forest as for the related clear-cut.

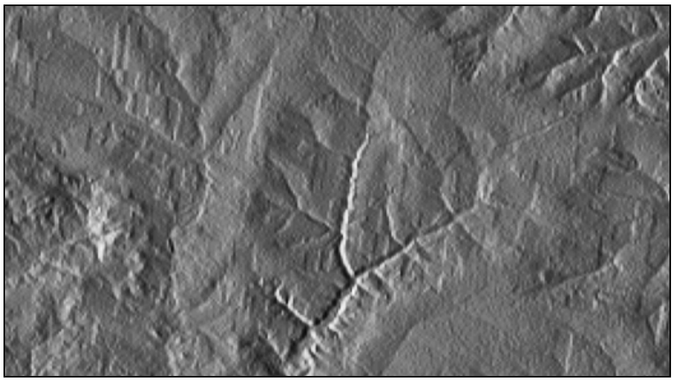

Figure 20. Clear-cuts visible at shaded relief based on SRTM elevation data (Chunsky N)

Analogous to SRTM data also ALOS PALSAR interferograms are affected by forest in terms of adding a height term to the surface elevation. Fig. 21 shows an example of an interferometric phase image. The dark rectangle in the middle of the image corresponds to a remaining patch of dense forest surrounded by clearings. Across that forest patch an intersection AB has been defined. The related interferometric phase profile is provided at Fig. 22. The offset of the interferometric phase ϕ at the southern wane is assigned with $\Delta\phi_{HH}$ *and* $\Delta\phi_{HH}$ respectively. Besides that fact that there is an offset in this example, this offset obviously differs for HH and HV. Main focus of this side study is put on this difference. However, major interest exists for the phase offset difference between winter and summer HH data.

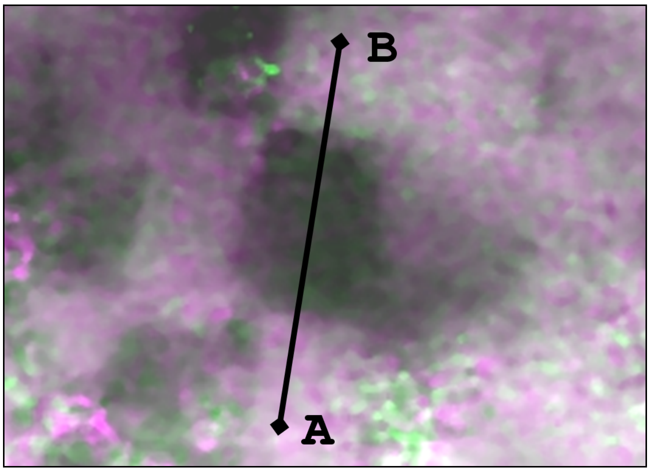

Figure 21. Interferometric phase for an area featuring forest and clear-cuts (RGB = ϕHH ϕHV ϕHH)

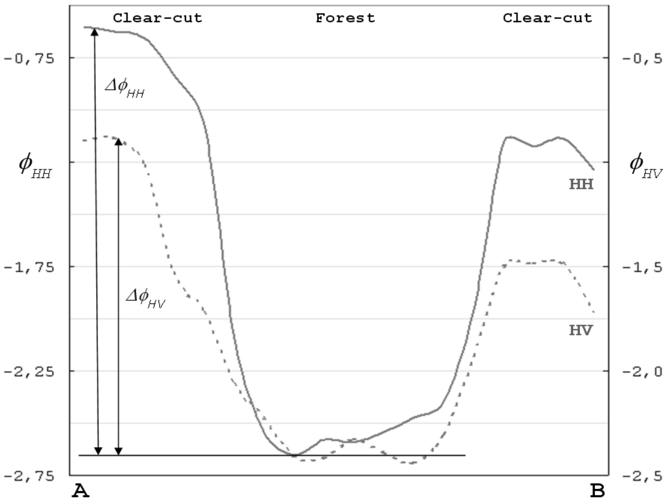

Figure 22. Smoothed interferometric phase profile for intersection at Fig. 21

The interferometric phase offsets were scaled to meters by applying Eq. (2). In this equation the height offset Δh is determined by $\Delta\phi$ - the interferometric phase offset, λ is the wavelength, R corresponds to the slant range distance, θ corresponds to the incidence angle, and B_{perp} to the perpendicular baseline. Being independent of the baseline the measurements from all interferograms can be compared.

$$\Delta h = \frac{\Delta\phi \cdot \lambda \cdot R \cdot \sin\theta}{4\pi \cdot B_{perp}} \tag{2}$$

In the majority of cases, more than one expedient interferogram was available per season (summer and winter). In those cases, the interferometric phase offsets have been investigated for all possible combinations of summer and winter interferograms (compare Fig. 23 & 24).

In order to avoid unwrapping effort the investigation was conducted with unwrapped interferograms. Hence, the forest patch as well as the related clear-cut must be located within one INSAR phase cycle (fringe). For both, the forest patch and the clear-cut a representative area close to the wane, each covering 200-400 pixels, was selected manually. The selection was based on forest inventory data and high resolution optical and SAR data (TerraSAR-X) and considered the masking criteria from above. Due to the low coherence at dense forest areas (only winter pairs have been affected) the whole approach was somewhat limited. Still, quite a number of wanes could be detected, whereas the wanes at the high stem volume forests are lost. For each representative area the average phase has been computed.

The following two diagrams (Fig. 23 & 24) summarise the results of the phase analysis. The first one compares the phase centre offset of HH summer against HH winter interferograms. Although the relative offset is biased by topography (this bias can unfortunately not be corrected for, as no topographic surface model is available), a clear trend is visible. Furthermore, the absolute offset (difference) is unaffected by this error source. Although the trend is not very significant, the phase offset in summer is about two times larger than in winter. The maximum offset in summer is about 37 m, whereas only 18 m are measured for the same wanes in winter. As only those wanes were considered, were the SRTM data features greater elevation for forest as for the related clear-cut, merely positive offsets emerge. Even affected by some uncertainties, Fig. 23 proves the greater penetration of the SAR wave during winter. Fig. 24 shows the same dataset, however by means of employing the summer-winter offset difference. This emphasises the significant phase offset at the wanes during summer. The minor impact of the winter offset results in a high remaining autocorrelation proportion of $\Delta\phi HH_{Summer}$.

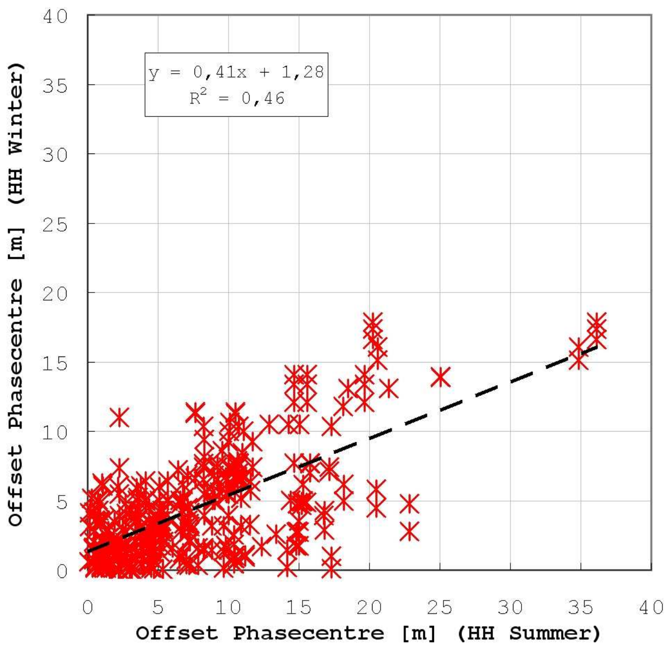

Figure 23. Offset ϕ at wanes, summarised for all sites (320 entities): $\Delta\phi HH_{Summer}$ vs. $\Delta\phi HH_{Winter}$

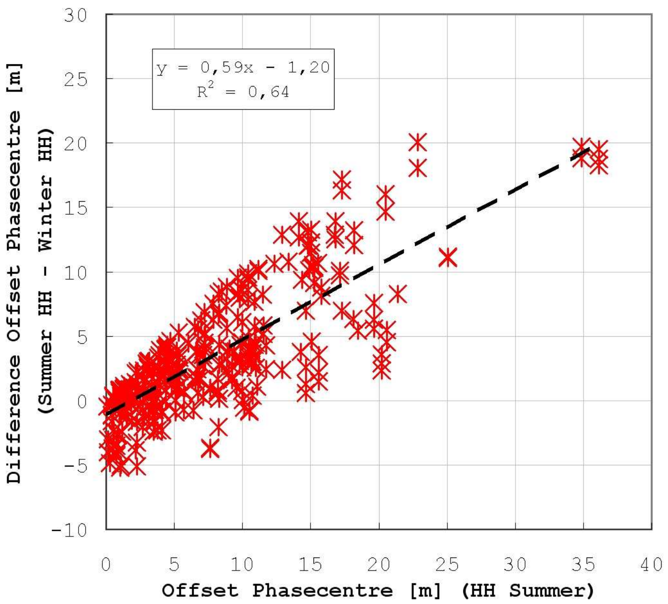

Figure 24. Offset ϕ at wanes, summarised for all sites (320 entities): $\Delta\phi HH_{Summer}$ vs. $\Delta\phi HH_{Summer}$ - $\Delta\phi HH_{Winter}$

As side product, Fig. 25 provides a comparison of phase offsets for HH and HV polarisation; both acquired simultaneously (summer data). Surprisingly, the phase offsets do not differ significantly. As volume scattering – producing a high cross polarisation term – is usually linked to the forest canopy, one could have expected an increased phase centre against HH, were the scattering at L-band is generated by stem-ground like interactions. However, even the HH phase centre seems being located in the upper forest layer.

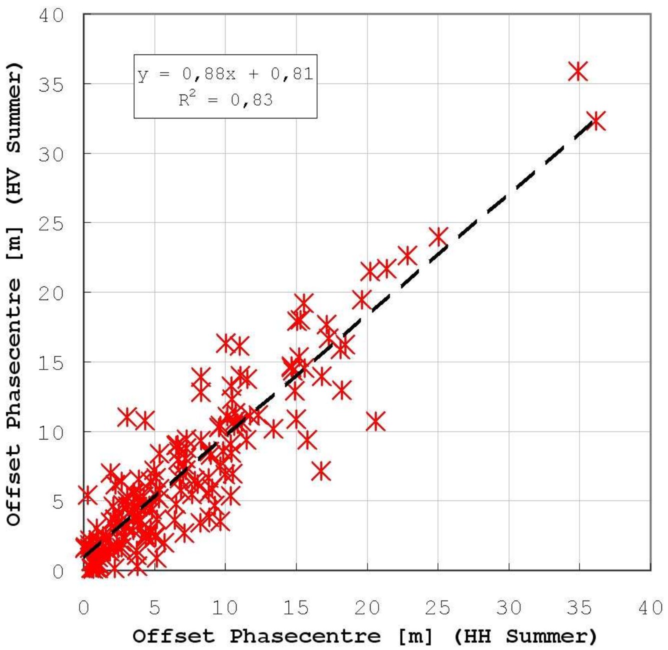

Figure 25. Offset ϕ at wanes, summarised for all sites: $\Delta\phi HH_{Summer}$ vs. $\Delta\phi HV_{Summer}$ (170 entities)

IV. Discussion

Besides the beneficial effect to learn more about L-band repeat pass coherence in the boreal zone and its suitability for stem volume retrieval, this study brought up an interesting and to some part unexpected aspect of the seasonal behaviour. For consecutive cycle coherence in summer obviously the overall temporal decorrelation is not larger than in winter. This surprisingly also applies to high stem volume classes. So far, the decorrelation of high stem volume areas is interpreted as effect of volumetric decorrelation. Temporal decorrelation is assumed to have minor effects (so far only winter coherence data have been applied to model the relationship between stem volume and L-band coherence; in winter we find extremely stable environmental conditions in Central Siberia).

The decrease of penetration depth into the canopy of the incoming SAR wave in summer, as proved by means of the phase analysis, could result in reduced volumetric decorrelation (raised and narrower scattering centre). Further evidence of this assumption could be seen in the remarkable examples, where increasing coherence with increasing stem volume was detected (Fig. 14), because potential changes in soil moisture in particular impacts areas with low stem volume and thus large penetration. Also the fact, that the HH phase centre for forest is vertically located close to the HV phase centre could indicate a high HH backscatter portion coming from the upper forest layer. A clear indicator for differing scattering processes in summer and winter is that coherence images, computed by means of one summer and one winter image, feature almost complete decorrelation for the whole frame, except some forest free patches. Thus, even there are changing soil conditions, some correlation remains. At forested areas however complete decorrelation is measured.

Besides the differing temporal decorrelation the larger spread of summer coherence could be caused by differing tree geometries, which are related to diverse tree types. In winter, the trees are semitransparent; twigs and branches can be expected to hardly impact the backscatter. Thus, all tree types are more or less equal targets, as the stem is the only part being able to interact with the radar wave.

Another very meaningful issue arises from the investigation of the perpendicular baseline effect on the coherence over dense forest. For winter coherence no impact of spatial baseline was evident. This introduces another big advantage of winter coherence for stem volume retrieval, even though the reason of this behaviour is not yet fully clear. One possible explanation, which is in accordance with all above results, is as follows: The frozen forest, represented by stems and canopy, is a semitransparent layer on top of the surface. This layer introduces a noise component to the coherent signal coming from the ground (point- and surface scattering). The amount of noise is driven by the density and the depth of this forest layer, which is in turn a function of stem volume. Basing on this assumption the coherence modelling over forest becomes rather simple.

The statements above are based on initial interpretations and more work has to be done to completely understand the seasonality of coherence and backscatter in the boreal zone. In particular, backscatter models need to consider this variable. Further and more meaningful results could be delineated based on polarimetric data. However, so far no suitable datasets are available.

V. Conclusions and Outlook

ALOS PALSAR data proved having great potential for forest stem volume estimation in Siberia. Winter FBS coherence is the most powerful measure. Summer FBD coherence can provide additional information (e.g. for forest cover mapping), but the temporal baseline must be enlarged to increase temporal decorrelation of forest. However, this approach is very susceptible to variable environmental conditions. The computation of coherence based on FBS (winter) and FBD (summer) images is technically feasible but not very useful; it might - if at all - be used to support forest cover mapping.

With regards to the high summer coherence at dense forest, some evidence for a potentially reduced volumetric decorrelation has been discovered. In particular the reduced penetration in summer at forested areas supports this assumption.

So far, the effect of forest types has not been considered. This will be done in future and is of particular interest regarding summer coherence data.

References

[1] D.G. Leckie & K.J. Ranson, "Forestry applications using imaging radar", (Eds. F.M. Henderson & A.J. Lewis. "Principles and applications of imaging radar"), 3rd edn. Wiley, New York: 435-510, 1998.

[2] E. Kasischke, L. Bourgeau-Chavez, N. French, P. Harrell & N. Christensen, "Initial observations on using SAR to monitor wildfire scars in boreal forests", Int. J. Remote Sensing 13(18): 3495-3501, 1992.

[3] S.M. Yatabe & D.G. Leckie, "Clearcut and forest-type discrimination in satellite SAR imagery", Canadian J. Remote Sensing 21(4): 456-467, 1995.

[4] E. Rignot, W.A. Salas & D.A. Skole, "Mapping deforestation and secondary growth in Rondonia, Brazil, using imaging radar and thematic mapper data", Remote Sensing Env. 59: 167-179, 1997.

[5] C. Thiel, P. Drezet, C. Weise, S. Quegan & C. Schmullius, "Radar Remote Sensing for the Delineation of Forest Cover Maps and the Detection of Deforestation", Forestry - An International Journal of Forest Research 79 (5): 590-597, 2006

[6] Ch. Thiel, Ca. Thiel & C. Schmullius, "Operational Large Area Forest Monitoring in Siberia Using ALOS PALSAR Summer Intensities and Winter Coherence". IEEE Trans. Geosc. and Rem. Sens. 47 (12): 3993-4000, 2009.

[7] M.C. Dobson, F.T. Ulaby, T. Le Toan, A. Beaudoin, E.S. Kasischke & N. Christensen, "Dependence of radar backscatter on coniferous forest biomass", IEEE Trans. Geosc. and Rem. Sens. 30(2): 412-415, 1992.

[8] H. Israelsson, J. Askne & R. Sylvander, "Potential of SAR for forest bole volume estimation", Int. J. Remote Sensing 15 (14): 2809-2826, 1994.

[9] M. Santoro, L. Eriksson, J. Askne & C. Schmullius, "Assessment of stand-wise stem volume retrieval in boreal forest from JERS-1 L-band SAR backscatter", Int. J. Remote Sensing 27: 3425-3454, 2006.

[10] J. Askne, M. Santoro, G. Smith & J.E.S. Fransson, "Multitemporal Repeat-Pass SAR Interferometry of Boreal Forests", IEEE Trans. Geosc. and Rem. Sens. 41 (7): 1540-1550, 2003.

[11] L.E.B. Eriksson, M. Santoro, A. Wiesmann & C. Schmullius, "Multitemporal JERS Repeat-Pass Coherence for Growing-Stock Volume Estimation of Siberian Forest", IEEE Trans. Geosc. and Rem. Sens. 41 (7): 1561-1570, 2003.

[12] M. Santoro, J. Askne, G. Smith & J.E.S. Fransson, "Stem volume retrieval in boreal forests from ERS-1/2 interferometry", Remote Sens. Env. 81: 19-35, 2002.

[13] J. Pulliainen, M. Engdahl & M. Hallikainen, "Feasibility of multi-temporal interferometric SAR data for stand-level estimation of boreal forest stem volume", Remote Sens. Env. 85: 397-409, 2003.

[14] J.T. Koskinen, J.T. Pulliainen, J.M. Hyyppä, M.E. Engdahl & M.T. Hallikainen, "The Seasonal Behaviour of Interferometric Coherence in Boreal Forest", IEEE Trans. Geosc. and Rem. Sens. 39 (4): 820-829, 2003.

[15] Ch. Thiel, Ca. Thiel, J. Reiche, R. Leiterer & C. Schmullius, "Analysis of ASAR and PALSAR data for Optimising Forest Cover Mapping – A GSE Forest Monitoring Study", Proc. of ForestSat 2007, 05. – 07. November, Montpellier, France, 2007.

[16] M. Santoro, C. Werner, U. Wegmüller & O. Cartus, "Improvement of interferometric SAR coherence estimates by slope-adaptive range common band filtering", Proc. IGARSS, Barcelona, Spain, 2007.

[17] U. Wegmüller, C. Werner & T. Strozzi, "SAR interferometric and differential interferometric processing", Proc. IGARSS, Seattle, USA, IEEE Publications: 1106-1108, 1998.

[18] Ch. Thiel & C. Schmullius, "Examination of Multi-Seasonal ALOS PALSAR Interferometric Coherence for Forestry Applications in the Boreal Zone", Proc. 3rd Joint PI Symposium of ALOS Data Nodes for ALOS Science Program, 09. – 13. November 2009, Kona, USA.

[19] J. Askne & M. Santoro, "Multitemporal Repeat Pass SAR Interferometry of Boreal Forests", IEEE Trans. Geosc. and Rem. Sens. 43 (6): 1219-1228, 2005.

[20] R.M. Goldstein & C.L. Werner, "Radar interferogram filtering for geophysical applications", Geophysical Research Letters, 25 (21): 4035-4038, 1998.

Acknowledgements

This work has been undertaken within the framework of the JAXA Kyoto & Carbon Initiative. ALOS PALSAR data have been provided by JAXA EORC. The authors thank Gamma RS for their support and Stefano Tebaldini for the fruitful discussion initiated at the BIOMASS workshop in Paris 2010.

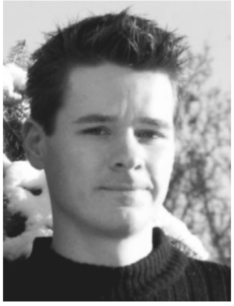

Christian J. Thiel received the Dipl. degree from the Friedrich Schiller University of Jena, Germany, in 2000 and the Ph.D. degree (with honours) from the Friedrich Schiller University of Jena, Germany, in 2004. Topic of his Ph.D. work was the investigation of polarimetric and interferometric airborne SAR data for the derivation of biophysical parameters. Since 2004 he works as Research Project Assistant and was involved in various projects. Subject-matters have been the synergistic usage of optical and SAR-data for landcover classification, earth observation in support for transboundary aquifer management, utilisation of JERS-1 SAR-data for forest cover detection, and the operationalisation of earth observation based forestry applications. Dr. Thiel is also involved in the Kyoto and Carbon Initiative, dealing with large area PALSAR data applications focussing on forest.

Since 2006 he is chair assistant at the Earth Observation Department of the Friedrich-Schiller University Jena and head of the Radar Science and Applications section. His main scientific interests are the development and application of methods for retrieving geophysical parameters over land from active remote sensing data with a particular interest in soil moisture retrieval, forest cover mapping, and forest biomass assessment.

Christiane C. Schmullius received the M.A. degree in geography/remote sensing from the University of California, Santa Barbara, in 1986 as an ITT and Fulbright Fellow and the Ph.D. degree from the Institute of Space Sciences, Free University Berlin, Germany, in 1991.

Her doctoral work focused on radar remote sensing of agricultural crops. From 1991 to 2000, she lead the “Geomatics”-group at the Institute for Radar Systems of the German Aerospace Center, DLR. In 1994, she coordinated the SIR-C/X-SAR Science Team and in 2000 became DLR’s Project Scientist for the Shuttle Radar Topography Mission (SRTM). She has coordinated several European Commission projects in Siberia, especially on radar interferometry applications for vegetation structure mapping. Since 2000, she is Professor for Earth Observation at the Friedrich Schiller University Jena, Germany, where she is focusing on synergetic optical-radar applications for large-scale land surface mapping.

Prof. Schmullius is a member of the following panels: Earth Science Advisory Committee of the European Space Agency, Space Advisory Group to the European Commission, European Space Science Council of the European Science Foundation.